Observation of skull-guided acoustic waves in a water-immersed murine skull using optoacoustic excitation

Héctor Estrada[a], Johannes Rebling[a,b], and Daniel Razansky[a,b]

[a]Institute for Biological and Medical Imaging (IBMI), Helmholtz Zentrum München, Germany
[b]School of Medicine and School of Electrical Engineering and Information Technology, Technical University of Munich, Germany

ABSTRACT

The skull bone, a curved solid multilayered plate protecting the brain, constitutes a big challenge for the use of ultrasound-mediated techniques in neuroscience. Ultrasound waves incident from water or soft biological tissue are mostly reflected when impinging on the skull. To this end, skull properties have been characterized for both high intensity focused ultrasound (HIFU) operating in the narrowband far-field regime and optoacoustic imaging applications. Yet, no study has been conducted to characterize the near-field of water immersed skulls.

We used the thermoelastic effect with a 532 nm pulsed laser to trigger a wide range of broad-band ultrasound modes in a mouse skull. In order to capture the waves propagating in the near-field, a thin hydrophone was scanned in close proximity to the skull's surface. While Leaky pseudo-Lamb waves and grazing-angle bulk water waves are clearly visible in the spatio-temporal data, we were only able to identify skull-guided acoustic waves after dispersion analysis in the wavenumber-frequency space. The experimental data was found to be in a reasonable agreement with a flat multilayered plate model.

Keywords: optoacoustic, photoacoustic, mouse skull, neuroimaging, acoustic guided waves, Lamb waves, laser ultrasonics

1. INTRODUCTION

The skull, a solid multilayered bone plate protecting the brain, poses a challenge for the use of ultrasonic waves in neuroscience. Ultrasound waves are strongly reflected when impinge on the skull[1] due to its acoustic properties, which have been characterized for focusing ultrasound deep inside the human brain[2–7] or to visualize the mouse brain vasculature[8,9] by means of optoacoustic microscopy. The mentioned studies made use of sources/receivers placed at the skull's far-field. Here we explore the near-field of a mouse skull by directly exciting ultrasonic waves by optoacoustic means and scanning a needle hydrophone close to the skull.

2. METHODS

To access the skull's near-field, one has to deal with the problem of the skull curvature. We overcome this problem by performing a preliminary ultrasound pulse-echo scan of the skull (see Fig. 1(a)) using a focused PVdF transducer (30 MHz, Precision Acoustics, UK). The geometry of the 6 weeks old mouse skull is extracted from the ultrasonic data and used to perform the near-field's scan using a needle hydrophone (0.5 mm in diameter, PVdF, Precision Acoustics, UK) following the skull's curved surface (see Fig. 1(b)).

Direct excitation ultrasound waves in the skull by optical means is not efficient due to the low light absorption of bone. Therefore, the target is a thin layer of black burnish on the skull's interior surface which acts as the ultrasound source due to the thermoelastic effect (see Fig. 1 (b)). The absorbing target is illuminated with 532 nm pulsed light generated by a Q-switched diode laser (EdgeWave GmbH, Germany) having a per-pulse energy of 3 μJ and a duration of 10 ns. The skull was immersed in a phosphate buffered saline (PBS) solution (Life Technologies Corp., UK) before and during the experiments.

Further author information: (Send correspondence to D.R.)
D.R.: E-mail: dr@tum.de

Optical Elastography and Tissue Biomechanics IV, edited by Kirill V. Larin, David D. Sampson, Proc. of SPIE Vol. 10067, 1006710 · © 2017 SPIE · CCC code: 1605-7422/17/$18 · doi: 10.1117/12.2252089

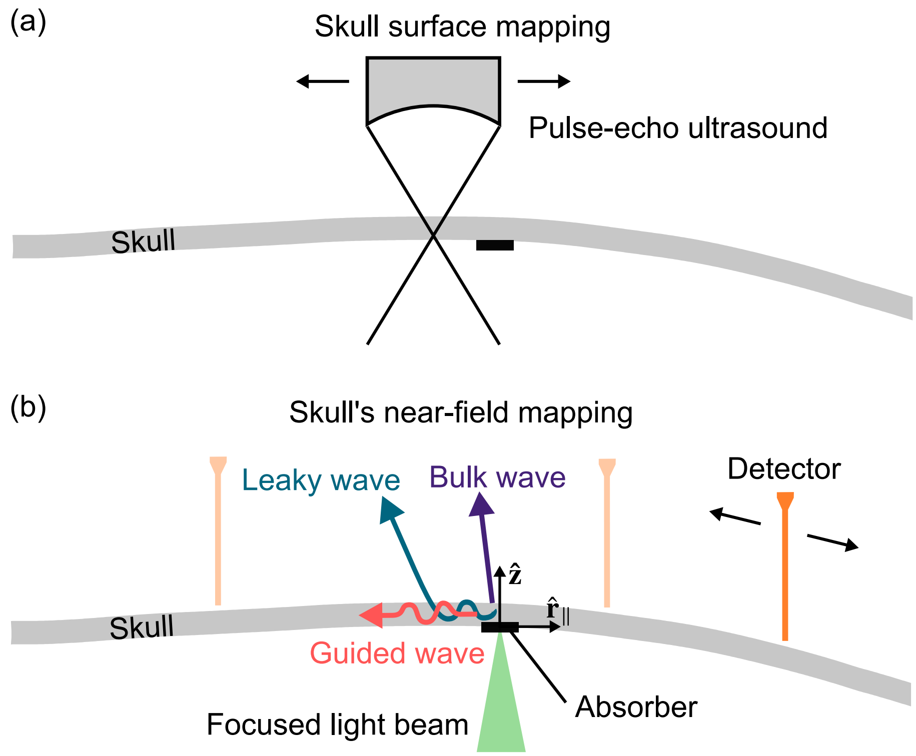

Figure 1. (a) Measurement of the skull's geometry using pulse-echo ultrasound. (b) Near-field mapping of the skull using an hydrophone and laser excitation.

3. RESULTS

Using short-pulse laser excitation, we are able to simultaneously trigger different kinds of wave (see Fig. 1(b)). As the skull is immersed in a fluid, we will observe supersonic (relative to the fluid) waves leaving (hence leaky-wave) the skull after shortly propagating through it a given angle. Also bulk ultrasound waves are radiated to the fluid. If the phase velocity of a wave in the skull is smaller than the phase velocity in the fluid, then the wave is guided by the skull and cannot be radiated to the far-field. If a skull-guided wave exists, it should only be detectable at the skull's near-field. The measured wave propagation as a function of the distance to the source and the time of flight (see Fig. 2(a)) clearly shows the leaky and the bulk radiated waves. As expected, the leaky waves are barely visible beyond 1 μs because they leave the near-field. Bulk waves closely follow the sound line (speed of sound in the fluid $c_0 = 1502$ m/s). Although the wave amplitude is represented in logarithmic scale, skull-guided waves are not visible in this plot. Before concluding that no skull-guided waves were detected, we can disentangle the information contained in Fig. 2(a) by applying a two-dimensional Fourier transform, shown in Fig. 2(b). The reciprocal space representation separates the far-field $\omega > c_0 k_{\parallel}$[*] from the near-field $\omega < c_0 k_{\parallel}$ with a line given by $\omega = c_0 k_{\parallel}$ which represents a wave propagating parallel to the skull at the speed of sound in the fluid c_0. As predicted by a flat plate model,[10] a subsonic mode appears below the sound line in both propagation directions (see Fig. 2(b)). The spectrum is, however, not symmetric due to the skull's inhomogeneities and curvature. The nature of the subsonic modes seems similar to Lamb-Rayleigh waves,[11] in particular to the cutoff-free antisymmetric mode, also known as A_0. In order to see how the subsonic Lamb-like modes look in space-time, we can choose a window in reciprocal space (indicated in red in Fig. 2(b)) and assign zeros to anything outside the selected region and perform an inverse two-dimensional Fourier transform. Figure 2(c) shows the propagation of the skull-guided modes.

[*] ω represents the radial frequency and $k_{\parallel}$ the wavenumber parallel to the skull.

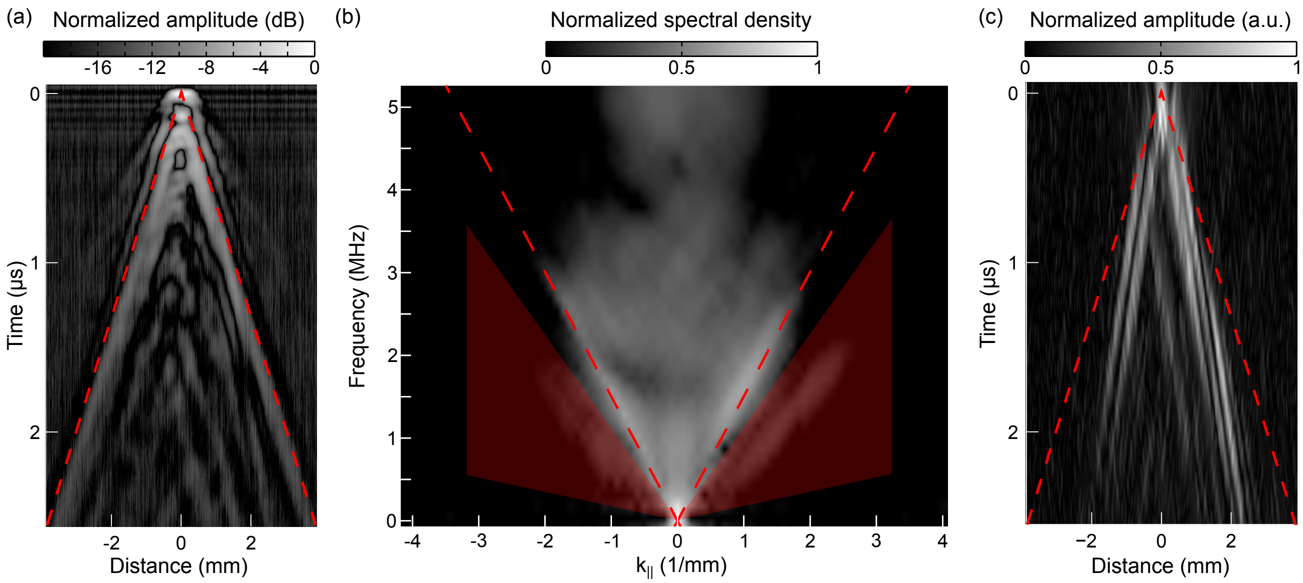

Figure 2. (a) Measured signal amplitude as a function of the distance to the source across the hydrophone scanning path and the time of flight. (b) Normalized spectral density after applying two-dimensional Fourier transform to the data on (a) as a function of the parallel-to-the-skull wavenumber and the frequency. The shadowed red region depicts the spectral window on which an inverse two-dimensional Fourier transform is applied to eventually obtain (c), which shows the signal amplitude of the skull-guided waves as a function of the distance relative to the source and the time of flight. The dashed red line represents the speed of sound in the immersion medium in both, real and reciprocal space.

4. CONCLUSIONS

We present experimental evidence on the existence of skull-guided waves for a murine skull immersed in water. The use of complementary imaging techniques allowed us to scan an ultrasound detector following the irregular shape of the skull and thus, access the skull's near-field. Direct optoacoustic excitation of the skull revealed helpful to trigger different wave propagation paths covering a relatively broad ultrasonic bandwidth. In addition, reciprocal-space analysis played a key role in the identification of the skull-guided waves. We hope our work could stimulate further research on skull-guided waves and its use in neuroscience.

ACKNOWLEDGMENTS

The research leading to these results has received funding from the European Research Council under grant agreement ERC-2015-CoG-682379. D. R. and J. R. acknowledge support from the European Research Council through the Initial Training Network Grant Nr. 317526.

REFERENCES

[1] Fry, F. J. and Barger, J. E., "Acoustical properties of the human skull," *The Journal of the Acoustical Society of America* **63**(5), 1576–1590 (1978).

[2] Clement, G. T. and Hynynen, K., "A non-invasive method for focusing ultrasound through the human skull," *Physics in Medicine and Biology* **47**(8), 1219 (2002).

[3] Clement, G. and Hynynen, K., "Correlation of ultrasound phase with physical skull properties," *Ultrasound in Medicine & Biology* **28**(5), 617 – 624 (2002).

[4] Clement, G. T., White, P. J., and Hynynen, K., "Enhanced ultrasound transmission through the human skull using shear mode conversion," *The Journal of the Acoustical Society of America* **115**(3), 1356–1364 (2004).

[5] Marquet, F., Pernot, M., Aubry, J.-F., Montaldo, G., Marsac, L., Tanter, M., and Fink, M., "Non-invasive transcranial ultrasound therapy based on a 3d ct scan: protocol validation and in vitro results," *Physics in Medicine and Biology* **54**(9), 2597 (2009).

[6] Pichardo, S., Sin, V. W., and Hynynen, K., "Multi-frequency characterization of the speed of sound and attenuation coefficient for longitudinal transmission of freshly excised human skulls," *Physics in Medicine and Biology* **56**(1), 219 (2011).

[7] Pinton, G., Aubry, J.-F., Bossy, E., Muller, M., Pernot, M., and Tanter, M., "Attenuation, scattering, and absorption of ultrasound in the skull bone," *Medical Physics* **39**(1), 299–307 (2012).

[8] Kneipp, M., Turner, J., Estrada, H., Rebling, J., Shoham, S., and Razansky, D., "Effects of the murine skull in optoacoustic brain microscopy," *Journal of Biophotonics* **9**(1-2), 117–123 (2016).

[9] Estrada, H., Rebling, J., Turner, J., and Razansky, D., "Broadband acoustic properties of a murine skull," *Physics in Medicine and Biology* **61**(5), 1932 (2016).

[10] Estrada, H., Rebling, J., and Razansky, D., "Prediction and near-field observation of skull-guided acoustic waves," *ArXiv e-prints* (June 2016).

[11] Royer, D. and Dieulesaint, E., [*Elastic Waves in Solids*], vol. I, Springer-Verlag Berlin Heidelberg New York (2000).